Loop Dependence of the Dynamics of DNA Hairpins

ARTICLE *in* THE JOURNAL OF PHYSICAL CHEMISTRY B · NOVEMBER 2001

Impact Factor: 3.3 · DOI: 10.1021/jp0121926

3 AUTHORS, INCLUDING:

Serguei Kuznetsov
University of Illinois at Chicago
40 PUBLICATIONS **673** CITATIONS
SEE PROFILE

Anjum Ansari
University of Illinois at Chicago
53 PUBLICATIONS **3,076** CITATIONS
SEE PROFILE

Loop Dependence of the Dynamics of DNA Hairpins

Yiqing Shen,[†] Serguei V. Kuznetsov,[†] and Anjum Ansari*[,†,‡]

Department of Physics (M/C 273) and Department of Bioengineering (M/C 063), University of Illinois at Chicago, 845 West Taylor Street, Chicago, Illinois 60607

Received: June 11, 2001; In Final Form: August 9, 2001

The kinetics of unwinding of DNA hairpins with varying loop sizes L was monitored using time-resolved absorbance measurements after a laser temperature jump. The characteristic time for forming hairpins is found to scale with the loop size as $L^{2.0\pm0.2}$, for loops consisting of both poly(dT) and poly(dA) strands, in close agreement with the scaling of loop-closure probability expected for semiflexible polymers. In contrast, equilibrium measurements show that the hairpins with smaller loops are stabilized by a factor that is much larger than can be accounted for simply by the entropic cost of bringing two ends of the polymer together. This excess stability of smaller loops partitions into the opening times, which are found to decrease as $L^{-2.0\pm0.3}$. The temperature dependence of the observed relaxation times, together with the equilibrium measurements, yields negative activation energy ($\approx -11 \pm 2.3$ kcal/mol) for the closing step at temperatures near the melting temperature of the hairpins. In contrast, temperature dependence of the relaxation times, obtained primarily at temperatures below the melting temperature from fluctuation correlation spectroscopy measurements on similar hairpins, yield activation energies for the closing step that are positive (Bonnet, G.; Krichevsky, O.; Libchaber, A. *Proc. Natl. Acad. Sci. U.S.A.* **1998**, *95*, 8602; Goddard, N. L.; Bonnet, G.; Krichevsky, O.; Libchaber, A. *Phys. Rev. Lett.* **2000**, *85*, 2400). A configurational diffusion model to describe hairpin dynamics is presented in which transient trapping in misfolded loops is sufficient to explain the change in the sign of the activation energy in the two sets of measurements.

Introduction

Hairpin formation in single-stranded DNA (ssDNA) is known to play a key role in many biological functions such as gene expression, DNA recombination, and DNA transposition.[1−3] In RNA, hairpins form at various sites along the polynucleotide and serve as nucleating centers for the subsequent folding of the RNA into its final three-dimensional conformation. The thermodynamics and kinetics of hairpin formation has been studied extensively.[4−16] However, despite the more than 30 years of biophysical research on the hairpin-to-coil transition, there are many unresolved questions.

It is well-known that the stability of hairpins with identical stems and varying loops depends on the size and composition of the loop, with smaller loops stabilized by a factor that is much larger than can be accounted for by the variation in the entropic cost of loop closure.[8,9,13,16−18] This excess stability from loops in hairpins has been attributed to loop−stem stacking interactions.[8,9] However, there is no satisfying explanation for why the loop−stem stacking interactions should diminish with increasing loop size. Vallone and Benight[19] have suggested that the hydrophobic interactions of the bases within the loop, and the exclusion of water from tight loops, may be a significant factor in the stability of hairpins with small loops.

These equilibrium measurements raise the question as to how this excess stability of hairpins from loops partitions into the opening and closing times for the dynamics of hairpin formation. Kinetics measurements on hairpins with varying loop sizes are limited. In one such study, Libchaber and co-workers[20,21] monitored the opening and closing of DNA hairpins labeled with a fluorophore and a quencher using fluctuation correlation spectroscopy (FCS) as a tool. They found that the closing times scale with the length of the loop L as $\sim L^{2.6\pm0.3}$, with the scaling exponent increasing from about 2.3 to 2.9 as the temperature was decreased from about 33 °C to 10 °C. Their opening times were found to be independent of the loop size.

In the analysis of Libchaber and co-workers, the activation energies for the characteristic closing times were positive ($\gtrsim 5$ kcal/mol) and increased with increasing loop size for poly(dA) loops.[20,21] They interpreted their activation energies for the closing step as the energetic cost of forming loops. This interpretation is at odds with what is expected for a semiflexible polymer, for which the energetic cost of forming loops is expected to decrease with increasing loop length. On the basis of their results, Libchaber and co-workers have argued that a semiflexible polymer description of ssDNA is not valid.[21] They postulate that poly(dA) displays an enthalpic rigidity as a result of considerable base stacking and that, for loops made of longer poly(dA) strands, there is a larger extent of disruption of base stacking, thus increasing the energetic cost of forming loops.

The kinetics of the hairpin-to-coil transition has also been investigated using temperature-jump (T-jump) techniques by several groups.[6,8,9,18,22] The T-jump measurements are in apparent contradiction with the measurements of Libchaber and co-workers, in that the closing times yield negative activation energies (≈ -11 kcal/mol).[18,22] Negative activation energies have also been observed in the kinetics of duplex formation[23,24] as well as in the kinetics of formation of β-hairpins[25] and α-helices[26] in polypeptides.

Klenerman and co-workers, in another set of FCS measurements on hairpins with large poly(dA) loops, have shown that

* Corresponding author. E-mail: ansari@uic.edu. Phone: (312) 996-8735. Fax: (312) 996-9016.
† Department of Physics (M/C 273).
‡ Department of Bioengineering (M/C 063).

10.1021/jp0121926 CCC: $20.00
Published on Web 11/08/2001

the kinetics are nonexponential and have interpreted their results as arising from a distribution of opening and closing times.[27] Their data also show that the closing times for hairpin formation exhibit non-Arrhenius behavior.[28] Some deviations from an Arrhenius behavior were already observed in the measurements of Goddard et al.[21] Therefore, kinetics measurements over a wide temperature range show that the activation energy changes sign from positive values below the melting temperature to negative values when the temperature is increased above the melting temperatures. These results indicate that the simplest two-state description for the hairpin-to-coil transition, with Arrhenius dependences for the opening and closing times, is at best inadequate.

In this work we have measured the stability and kinetics of hairpins with 4−12 poly(dT) or poly(dA) bases in the loop, using time-resolved absorbance measurements to monitor the unwinding in response to laser T-jumps. We find that at temperatures near the melting temperature of the hairpins, the closing times for both poly(dT) loops and poly(dA) loops scale as $L^{2.0\pm0.2}$, in close agreement with polymer theories that predict an exponent of ≈1.8 for the loop-closure probability of a semiflexible polymer of lengths longer than a typical statistical segment length.[29] Our results show that a semiflexible polymer description is a reasonable first approximation for describing the dynamics of ssDNA segments even at these short length scales, and that this description becomes more accurate near the melting temperatures. In contrast to the observation of Libchaber and co-workers, we find that opening times also depend on the size of the loop, as is expected from the large dependence on loop size observed for the stabilizing free energy of the hairpins.

In an attempt to reconcile the discrepancies observed between our measurements and those of Libchaber and co-workers, we have modeled the dynamics of hairpin formation using a configurational diffusion model.[22] Our model reproduces the non-Arrhenius temperature dependence of the closing times, with the change in sign of the observed activation energy for the closing step. Our model also provides an explanation for why the scaling exponent describing the loop-size dependence of the closing times increases with decreasing temperature. A brief account of this discussion appears elsewhere.[30]

Experimental Section

Materials. The DNA oligomer strands were purchased from Oligos Etc. (Wilsonville, OR). All samples were HPLC purified. The buffer was 100 mM NaCL, 10 mM sodium phosphate, and 0.1 mM EDTA, pH 7.5. The strand concentrations in all experiments were less than 100 μM, well within the concentration range of up to 500−800 μM for which unimolecular hairpin formation is observed.[10,14]

Equilibrium Measurements. Optical melting profiles were obtained by measuring changes in the absorbance at 270 nm as a function of temperature. Absorbance measurements were done using a Hewlett-Packard 8452 (Palo Alto, CA) diode array single beam spectrophotometer equipped with a temperature controller. To convert the absorbance versus temperature profiles into a normalized absorbance that can be interpreted as the fraction of broken base-pairs $\theta(T)$, the absorbance profiles $A(T)$ were fitted to a two-state transition plus an upper (A_U) and a lower (A_L) baseline: $A(T) = \theta(T)[A_U(T) - A_L(T)] + A_L(T)$, where $\theta(T)$ is described in terms of a van't Hoff expression:

$$\theta(T) = \frac{1}{1 + \exp\left[-\frac{\Delta H}{R}\left(\frac{1}{T} - \frac{1}{T_m}\right)\right]} \quad (1)$$

Here ΔH is the enthalpy of a fully intact hairpin relative to the unwound (random coil) state, and is assumed to be temperature independent. T_m is the melting temperature of the hairpin. The upper and lower baselines were parametrized as straight lines with independently varying slopes.

Equilibrium "Zipper" Model. To describe the variation in the stability of the hairpin as a function of the size of the loop, we use an equilibrium "zipper" model in which the statistical weights of the microstates enumerating all partially unpaired hairpins (with the random coil chosen as the reference state) are written as[18]

$$z_{jk} = \sigma_{j,j+1}\left(\prod_{i=j+1}^{N_s-k} s_i\right) w_{loop}(N + 2k) \quad (2)$$

Here N_s is the total number of base-pairs in the stem, N is the number of bases in the loop of a fully intact hairpin, j is the number of broken base-pairs at the free end of the stem, and k is the number of broken base-pairs at the loop end of the stem. $\sigma_{j,j+1}$ is a cooperativity parameter that depends on the sequence.[12,18] If $j = 0$, the cooperativity parameter at the end of the hairpin is assigned a value of the average cooperativity parameter $\langle\sigma\rangle^{1/2}$ where $\langle\sigma\rangle = 4.5 \times 10^{-5}$.[31] s_i are the stability parameters for each base-pair and are defined with nearest-neighbor stacking interactions obtained from the work of Benight and co-workers.[12,32] $w_{loop}(n)$ is the end-loop weighting function for a loop of n ($=N + 2k$) bases.

End-Loop Weighting Function. The end-loop weighting function $w_{loop}(n)$ is written as

$$w_{loop}(n) = \left(\frac{3}{2\pi b^2}\right)^{3/2} V_r g(n) \sigma_{loop}(n) \quad (3)$$

Here b is the statistical segment length (also known as the Kuhn's length and equal to twice the persistence length P), V_r is a characteristic reaction volume within which the bases at the two ends of the loop can form hydrogen bonds, $g(n)$ is the loop-closure probability for a semiflexible polymer consisting of n monomers, and $\sigma_{loop}(n)$ describes the increase in the stability of the hairpin as a result of stabilizing free energy from the bases in the loop. The reaction volume V_r ($=4/3\pi r^3$) in eq 3 is calculated with $r = 1$ nm. In our calculations we obtain $g(n)$ from a wormlike chain model as derived by Yamakawa and Stockmayer.[33] The important feature of $g(n)$ that is important for our analysis is that $g(n)$ exhibits a maximum for loop lengths approximately one statistical segment long. For shorter loops $g(n)$ drops sharply because of the intrinsic rigidity of the polymer, and for longer loops it scales as $\sim n^{-1.5}$.[33−36]

As described in detail elsewhere,[18] we use two different functional forms to describe the dependence of $\sigma_{loop}(n)$ on the size of the loop. Both the functions incorporate the experimental result that the strength of the stabilizing interactions decrease as the loop size increases, and that, in the limit of infinitely large loops, $\sigma_{loop}(n)$ approaches the average value $\langle\sigma\rangle^{1/2}$. The two functional forms we tried are

$$\sigma_{loop}(n) = \langle\sigma\rangle^{1/2} + \frac{C_{loop}}{N_b^{\gamma}} \quad (4)$$

and

$$\sigma_{\text{loop}}(n) = \langle\sigma\rangle^{1/2} \exp\left(-\frac{D_{\text{loop}}/N_b^{\kappa}}{RT}\right) \quad (5)$$

The quantity $-RT \ln(C_{\text{loop}})$ in eq 4 (or D_{loop} in eq 5) is the free energy contribution to the stability of the hairpin from the loop for the most optimal loop size ($L \approx 2P$), N_b is the number of statistical segments in the loop $N_b = L/b = (n+1)h/b$, where h is the internucleotide distance and is assigned a value of 0.52 nm,[37] and γ in eq 4 (or κ in eq 5) describes the decrease in the stabilizing interactions with increasing loop size. The primary difference between the two functional forms is the approach to the large loop limit.

Fitting Procedure. The parameters P, C_{loop}, and γ (or P, D_{loop}, and κ) are varied to best describe the dependence of the melting temperatures on the loop size. To model the melting temperatures as a function of loop size, we first calculate the fraction of broken base-pairs as a function of temperature as described elsewhere.[18] The melting temperature from each theoretical melting profile is then compared with the experimental values. In principle, the theoretical melting profiles can be fit directly to the experimental melting profiles. In practice, the uncertainty in the a priori determination of the asymptotes complicates the direct fitting of the experimental melting profiles whereby the parameters describing the asymptotes need to be varied simultaneously with the end-loop parameters. The melting temperatures, on the other hand, are much less sensitive to the asymptotes and are well determined from the experimental data. In an earlier paper,[18] we fitted directly the absorbance melting profiles with a simultaneous fitting of the asymptotes. Parameters obtained from the simplified fitting procedure described here are essentially the same, to within the uncertainty in the parameters, as the ones obtained from fitting the absorbance profiles directly.

To ensure that we are not stuck in a local minimum and to check the robustness of the parameters, a simulated annealing procedure was used to sample the parameter space in order to minimize the residual sum-of-squares, starting from 20 independent randomly chosen sets of parameters.[38,39] The final parameters reported in the text are the best of 20 independent random searches, and the error bars in the parameters are the standard deviations obtained from a subset of the independent searches for which the residual sum-of-squares are within a factor of 3.

Temperature-Jump Apparatus. The T-jump spectrometer consists of a multimode Q-switched Nd:YAG laser (Continuum Surelite II, 600 mJ/pulse at 1.06 μm, full width at half-maximum $\approx$ 6 ns) that is used to pump a 2 m long Raman cell consisting of high-pressure methane gas.[22] The first Stokes line is separated from other wavelengths by a Pellen-Brocca prism. The conversion efficiency at 1.54 μm measured after the prism is 10−15% yielding ca. 60−80 mJ/pulse. The 1.54 μm beam is focused down to about 1 mm (full width at half-maximum) on one side of the sample cuvette with $\approx$300 μm path length. A typical T-jump achieved with this setup is about 10 °C. The probe source is a Xe/Hg 200 W lamp with a 10 cm water filter and an interference filter at 270 nm and is focused down to a spot size of $\lesssim$200 μm. The transmitted intensities are detected by a photomultiplier tube (Hamamatsu R928) with a 5 MHz current-to-voltage converter (Hamamatsu C1053−51), which has a gain of 300 mV/μA. The voltages are digitized using a 500 MHz transient digitizer (Hewlett-Packard 54825A).

Analysis of Kinetics Measurements. The observed kinetics at each temperature are fit to the functional form $[A(0^+,T_f) - A(\infty,T_f)]\exp(-t/\tau_r(T_f)) + A(\infty,T_f) + \delta A$. Here $A(\infty,T_f) + \delta A$ is the absorbance measured at times long compared to the relaxation time τ_r at the final temperature T_f, $A(0^+,T_f) + \delta A$ is the absorbance immediately after the laser pulse, and δA is the apparent change in the absorbance of the sample after the T-jump as a result of thermal lensing effects which introduce a constant offset in the absorbance data. δA is found to be $\approx$2 mOD as determined from the apparent change in absorbance measured in buffer alone. $A(0^+,T_f)$ is assumed identical to the pre-laser baseline absorbance $A(0^-,T_i)$ at the initial temperature T_i. The fitting parameters for each relaxation measurement are T_f and τ_r. In addition, since the variation in δA from one experiment to another is almost 100%, δA is also varied in order to optimize the fit. The parameter T_f is determined by the constraint that the amplitude of the kinetics signal $[A(0^+,T_f) - A(\infty,T_f)] = [A(0^-,T_i) - A(\infty,T_f)]$ has to match the amplitude $A(T_f) - A(T_i)$ determined from the absorbance melting profiles for a given pair of T_i and T_f.

Results and Discussion

Equilibrium Characterization of the Hairpin-to-Coil Transition. We have investigated the conformational dynamics of DNA hairpin as a function of loop length and loop sequence. Two sets of measurements were performed: (i) steady-state absorbance measurements to determine the equilibrium constant between the hairpin and random coil conformations and to extract the end-loop weighting function parameters and (ii) kinetics measurements that monitor hairpin formation, using time-resolved absorbance spectroscopy following a laser T-jump, to determine the characteristic relaxation times for the opening and closing of hairpins.

The absorbance of DNA hairpin loops increases with temperature as a result of both unstacking of the bases in the single-stranded regions (loop and random coils), as well as from unstacking of bases when the hydrogen bonds between base-pairs is broken. The first contribution results in an almost linear increase in absorbance at the low- and high-temperature ends of the melting profiles. The breaking of base-pairs, on the other hand, occurs in a cooperative manner (Figures 1 and 2). We have investigated the melting of six hairpins with identical stem and with poly(dT) or poly(dA) loops of varying sizes: 5′-CGGATAA(X_N)TTATCCG-3′ with X = A or T and N = 4, 8, or 12 bases. The absorbance changes corresponding to unstacking of single-stranded regions are much more apparent in the poly(dA) loops, with the slopes of the asymptotes increasing markedly with increasing loop length (Figure 2).

The equilibrium absorbance measurements are analyzed in terms of a two-state van't Hoff analysis (eq 1), with straight lines for the asymptotes, as described in the Experimental Section. The melting temperatures (T_m) and the enthalpy (ΔH) of hairpins relative to the random coil that best describe each of the melting profiles are summarized in Table 1. The T_m versus the number of bases in the loop, for the hairpins in this study, are plotted in Figure 3a. The T_m for another set of hairpins 5′-CCCAA(X_N)TTGGG-3′ (in 250 mM NaCl) with loop sizes ranging from N = 8−30, obtained from Goddard et al.,[21] are plotted in Figure 3b. The variation of T_m as a function of the loop size is modeled as described in the Experimental Section, with the end-loop weighting function parametrized as described in eqs 3−5. The parameters that best describe the dependence of T_m on the loop size are summarized in Table 2. The σ_{loop} parameters describe the enhanced stability of hairpins from stabilizing interactions within the loop, and the decrease in the strength of these interactions with increasing loop size. The loop dependence is the largest for hairpins with N ranging from 4 to

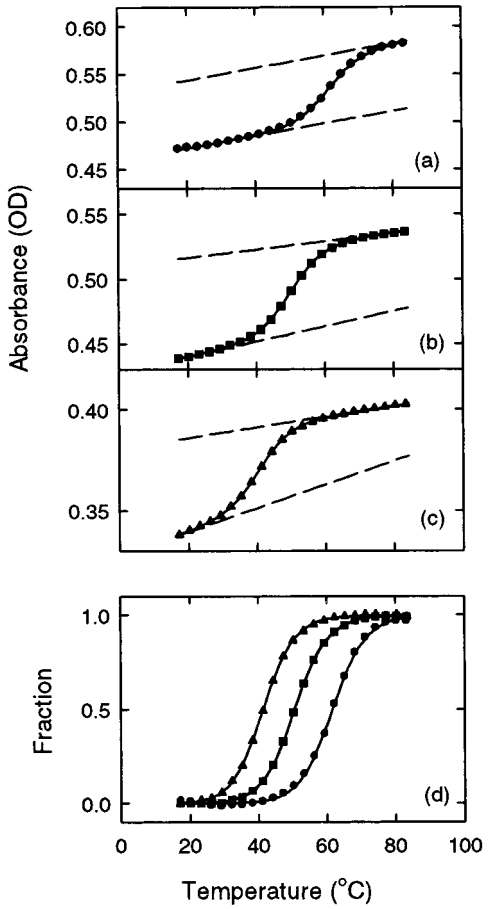

Figure 1. Melting profiles for the hairpin sequence 5′-CGGATAA-(T_N)TTATCCG-3′ with poly(dT) loops. (a−c) Absorbance at 270 nm is plotted against temperature for (a) $N = 4$, (b) $N = 8$, and (c) $N = 12$. The symbols are data points and represent the average of 20 data points obtained with a temperature resolution of 0.1 °C. The continuous lines are calculated by fitting to a two-state van't Hoff melting transition plus straight lines describing the high and low-temperature baselines (shown as dashed lines). The parameters describing the melting profiles are summarized in Table 1. (d) The normalized melting profiles after subtracting the baselines for (●) N = 4, (■) N = 8, and (▲) N = 12.

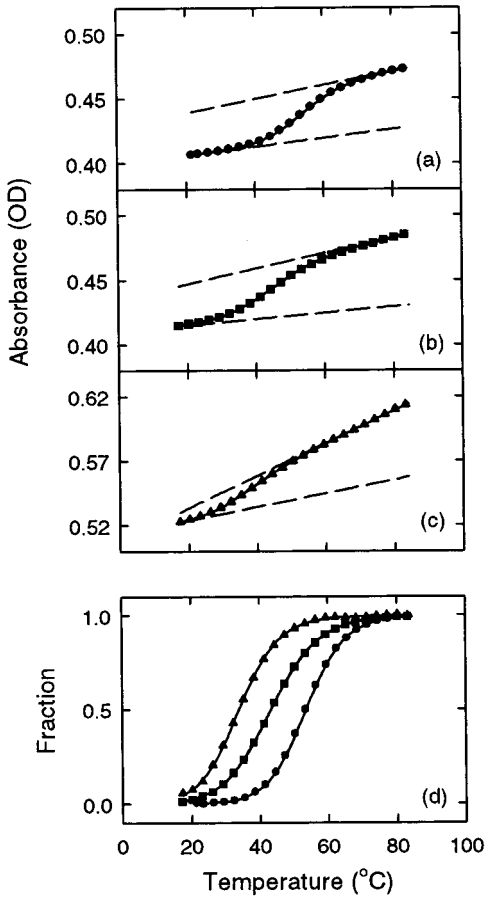

Figure 2. Melting profiles for the hairpin sequence 5′-CGGATAA-(A_N)TTATCCG-3′ with poly(dA) loops. (a−c) Absorbance at 270 nm is plotted against temperature for (a) $N = 4$, (b) $N = 8$, and (c) $N = 12$. (d) The normalized melting profiles after subtracting the baselines. The symbols and lines are as described for Figure 1.

TABLE 1: van't Hoff Parameters for Hairpins 5′-CGGATAA(X_N)TTATCCG-3′

X_N	T_4	T_8	T_{12}	A_4	A_8	A_{12}
ΔH (kcal/mol)	−40.8	−43.6	−42.8	−37.3	−28.8	−32.2
T_m (°C)	63.4	50.5	41.4	53.5	43.3	34

12 bases (Figure 3a), although the trend continues even for hairpins with N as large as 20−30 bases (Figure 3b).

Persistence Length of ssDNA. For hairpins with poly(dT) loops, our persistence length parameter P is in the range 1.5−1.7 nm, and the parameter is well determined for the different random searches and for the different functional forms picked for σ_{loop}. The exception is for the set of hairpins 5′-CCCAA-(T_N)TTGGG-3′ for which the smallest loop is with $N = 12$ bases (Figure 3b), which is significantly larger than a typical Kuhn's statistical segment length for poly(dT) strands in ssDNA. The parameters for this set of data are not very well determined. To estimate the persistence length from the dependence of T_m on loop size, it is important to include hairpins with loops of length close to the Kuhn's length. In an earlier paper[18] we had analyzed the melting temperatures of another set of hairpins with poly-(dT) loops, 5′-ATCCTA(T_N)TAGGAT-3′ with N ranging from 0 to 7 bases, obtained from Hilbers et al.;[8] a similar parametrization to describe the dependence of T_m on loop size yielded $P \approx 1.3-1.5$ nm. For poly(dA) loops, our values of P range from 1.8 to 2.5 nm.

It is instructive to compare our persistence length estimates with other estimates in the literature. Felsenfeld and co-workers[40] obtain values of the Flory characteristic ratio $C_\infty = \langle r \rangle^2/(nh^2) = b/h$, where $\langle r \rangle^2$ is the mean square end-to-end distance of the polymers, to be $C_\infty \approx 18$ in 2M NaCl for long poly(rU) strands. In their calculations, they use a value of $h = 0.15$ nm, which yields $b \approx 2.7$ nm and $P \approx 1.35$ nm. Tinland et al.[41] obtain $P \approx 1.3$ nm in 100 mM salt from measurements of the self-diffusion coefficients of ssDNA. The end-to-end distance measurements of single-stranded segments inserted between duplexes yield $P \approx 1.3-2.8$ nm.[42] Force-extension measurements of a single-stranded λDNA molecule yield $P \approx 0.75$ nm.[43] More recent measurements on the force-extension behavior of ssDNA have revealed deviations from the elastic properties of simple polymers, especially at the low ($\lesssim$10 pN) forces.[44] These deviations have been modeled as arising from partially formed hairpins in the low force regime; including the possibility of hairpin formation reproduces the measured curve down to $\approx$1 pN with $P \approx 1.6$ nm.[45] Measurements of rotational diffusion times of DNA duplexes with a central single-stranded region yield consistently larger values than our measurements with $P \approx 3.1$ nm for poly(dT) strands and $P \approx 7.8$ nm for poly(dA) strands at 4 °C.[37] The variation in persistence length values from these different measurements may well be a result of partially formed secondary structures in ssDNA. In our calculations we

TABLE 2: Parameters Describing the End-Loop Weighting Function

5′-stem(loop) of hairpin	P (nm)[a]	$-RT\ln(C_{loop})$[a] (kcal/mol)	γ[a]	P (nm)[b]	D_{loop}[b] (kcal/mol)	κ[b]
5′-CGGATAA(T_N)-3′	1.5 ± 0.3[c]	-2.7[d] ± 0.02	6.8 ± 0.1	1.6 ± 0.2	-7.3 ± 0.2	1.4 ± 0.2
5′-CGGATAA(A_N)-3′	1.8 ± 0.1	-1.2 ± 0.02	7.7 ± 0.3	1.8 ± 0.1	-5.6 ± 0.1	2.4 ± 0.1
5′-CCCAA(T_N)-3′	1 ± 0.3	-3 ± 1	2.7 ± 0.2	1.7 ± 0.4	-7.4 ± 0.9	0.52 ± 0.1
5′-CCCAA(A_N)-3′	2.3 ± 0.2	-2.7 ± 0.1	5.2 ± 0.2	2.5 ± 0.4	-6.6 ± 0.2	0.92 ± 0.1

[a] σ_{loop} is defined as in eq 4. [b] σ_{loop} is defined as in eq 5. [c] The values of the parameters are the best out of 20 independent random searches in parameter space. The indicated errors are estimated from deviations in the parameters from a subset of the independent searches for which the residual sum-of-squares increase by less than a factor of 3. [d] $T = 25$ °C for all values in this column.

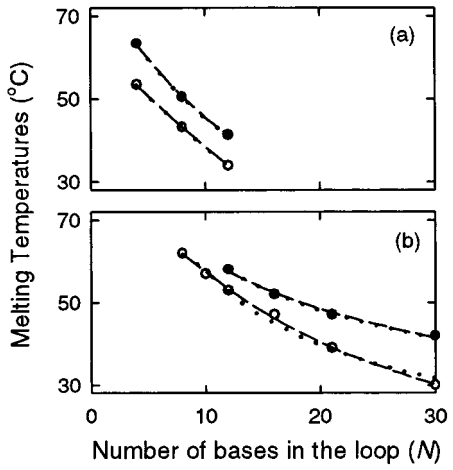

Figure 3. The melting temperature (T_m) versus number of bases (N) in the loop of a fully intact hairpin. (a) Hairpin sequence 5′-CGGATAA-(X_N)TTATCCG-3′ in 100 mM Na^+ with (●) T_N loops and (○) A_N loops. (b) Hairpin sequence 5′-CCCAA(X_N)TTGGG-3′ in 250 mM Na^+ with (●) T_N loops and (○) A_N loops. The melting temperatures are obtained from Goddard et al.[21] The continuous lines in parts a and b are the melting temperatures obtained from melting profiles calculated using the statistical mechanical "zipper" model, as described in the text, with σ_{loop} expressed as in eq 4 (dashed lines) and as in eq 5 (dotted lines). In part a the two fits are indistinguishable.

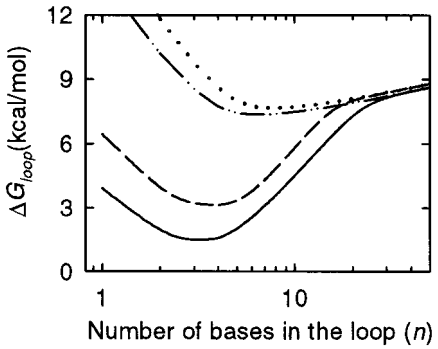

Figure 4. The free energy cost of loop formation. The curves are calculated from $\Delta G_{loop} = -RT\ln(w_{loop})$ where w_{loop} is expressed in terms of the wormlike chain model (eq 3) and the loop dependence of σ_{loop} is calculated using eq 4: (continuous line) poly(dT) loops, (dashed line) poly(dA) loops. The upper two curves are calculated with no stabilizing interactions from the loop in w_{loop} (i.e., with $C_{loop} = 0$ in eq 4): (dashed−dot-dot line) poly(dT) loops, (dotted line) poly(dA) loops.

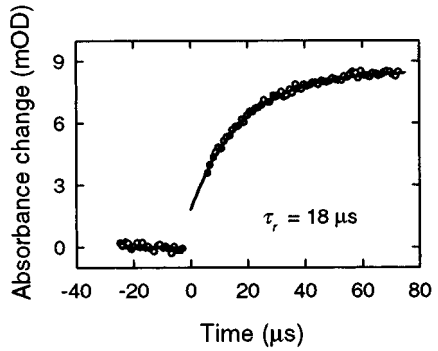

Figure 5. The change in absorbance as a function of time after a laser T-jump from 40 to 47 °C for the hairpin with $N = 8$ poly(dT) bases in the loop. The symbols are the measured data points. The continuous line is an exponential fit to the data with a relaxation time $\tau_r \approx 18$ μs. The absorbance signal does not extrapolate back to the preflash baseline because of an increase in the apparent absorbance after a T-jump and which is attributed to lensing effects from the heated volume.

exploit hairpin formation and explicitly include all partially formed hairpins in our enumeration of the microstates in the equilibrium "zipper" model.[18]

Our results that persistence lengths for poly(dA) loops are larger than that for poly(dT) loops are consistent with the observations of Mills et al.[37] The large variation observed in our values for the two sets of poly(dA) hairpins may arise from limitations in our model that assumes no temperature dependence for the persistence lengths. Felsenfeld and co-workers, in their light scattering and sedimentation velocity measurements of poly(rU) and poly(rA) fragments, have shown that although the radius of gyration of poly(rU) strands is nearly temperature independent between 18 and 40 °C, the radius of gyration of poly(rA) strands decreases by more than a factor of 2 in that temperature range.[40,46] Above about 40 °C, they find very similar values of C_∞ for both poly(rA) and poly(rU) segments. Their results on poly(rA) strands are consistent with a significant increase in the extent of stacking of poly(rA) bases at lower temperatures.[46] Therefore, for accurate modeling of the melting profiles for hairpins with poly(dA) loops, it may be necessary to include the temperature dependence of the persistence lengths.

Temperature-Jump Kinetics. The primary result from the equilibrium studies is that stabilizing interactions from the bases within the loop favor the formation of tighter loops by a factor that is by far a bigger contribution than the relative gain in entropic cost predicted for a semiflexible polymer (Figure 4). This result raises the question as to how the characteristic times corresponding to the closing and opening of hairpins scale with the size of the loop. To address this question we have monitored the kinetics of unwinding as a function of loop size, after a laser T-jump. The kinetics are monitored by measuring the change in absorbance at 265 nm as a function of time. A typical kinetic trace is shown in Figure 5 and is well described by a single-exponential in the time-window from about 5 μs to 500 μs (complete trace not shown). The relaxation times, obtained from an exponential fit to the kinetics, are found to be virtually independent of the loop size (data not shown). We use a two-state analysis to obtain the hairpin closing times (τ_c) and opening times (τ_o) from the measured relaxation times τ_r and the equilibrium constant $K_{eq} = (1 - \theta)/\theta$ where θ is obtained from the equilibrium melting profiles (Figures 1d and 2d):

$$\tau_c = \tau_r(1 + K_{eq})/K_{eq} \quad (6a)$$

$$\tau_o = \tau_r(1 + K_{eq}) \quad (6b)$$

The experimental results show that τ_c scales as $L^{2.2}$ for the poly-

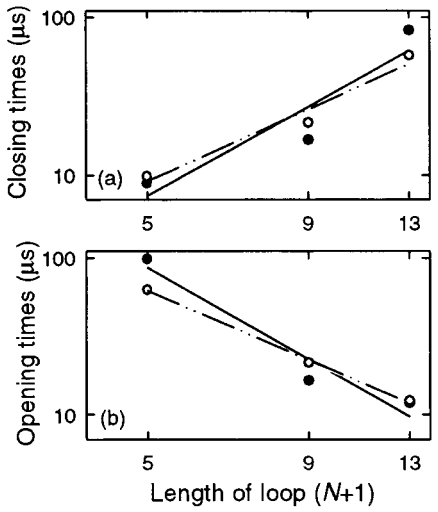

Figure 6. The closing times (τ_c) and the opening times (τ_o) versus the length of the loop. (a) Closing times for hairpins with poly(dT) loops (●) and poly(dA) loops (○). (b) Opening times for hairpins with poly-(dT) loops (●) and poly(dA) loops (○). The lines are fits to the data using the functional form $\tau_c \sim (N+1)^{\alpha}$ and $\tau_o \sim (N+1)^{-\beta}$. For poly-(dT) loops $\alpha = 2.2$ and $\beta = 2.3$ at $T \approx 51$ °C. For poly(dA) loops $\alpha = 1.8$ and $\beta = 1.7$ at $T \approx 43$ °C.

(dT) loops and as $L^{1.8}$ for the poly(dA) loops at temperatures close to the T_m of the hairpin with $N = 8$ bases in the loop (Figure 6). The important result here is that the exponent describing the scaling of the closing times with loop size is in close agreement with simple polymer theories, which predict an exponent of ≈1.8 for Gaussian chains with excluded volume.[29] These results indicate that, at least near the melting temperature, the dynamics of ssDNA are well described by a semiflexible polymer model for both poly(dT) and poly(dA) strands. The excess stability of the hairpins with smaller loops is reflected in the opening times, which are found to scale as $L^{-2.3}$ for poly(dT) loops and as $L^{-1.7}$ for poly(dA) loops.

Temperature Dependence of the Relaxation Times. We have also measured the temperature dependence of the relaxation times for the hairpin with $N = 8$ poly(dT) bases in the loop. Arrhenius plots for the relaxation times are shown in Figure 7. The observed relaxation times show a weak temperature dependence. We can rearrange eq 6a to give $\tau_r(T) = \tau_c K_{eq}/(1 + K_{eq})$. If we assume that $\tau_c(T)$ follows an Arrhenius temperature dependence with a viscosity-dependent preexponential, we can write

$$\tau_r(T) = \tau_{c0}(T_0)\frac{\eta(T)}{\eta(T_0)}\exp\left(\frac{\Delta H_c}{RT}\right)\left(\frac{K_{eq}}{1+K_{eq}}\right) \qquad (7)$$

Here τ_{c0} is the characteristic closing time at some reference temperature T_0 (=25 °C), η is the solvent viscosity and ΔH_c is the activation energy for the hairpin closing step. A fit to the relaxation times yields $\tau_{c0} = 10.7 \pm 2.6$ μs and $\Delta H_c = -10.9 \pm 2.3$ kcal/mol.[47]

Negative activation energies of ≈ −11 kcal/mol for the hairpin closing step were obtained for another set of hairpins in which the unwinding was monitored using fluorescence changes of 2-aminopurine, a fluorescent analogue of the adenine base, substituted instead of adenine at various sites along the stem of the hairpin.[18,22] Klenerman and co-workers have also reported negative activation energies of ≈ −13 kcal/mol for the closing of hairpins at temperatures above the melting temperature.[28] Negative activation energies have also been measured for duplex formation from complimentary strands of ssDNA,[23,24]

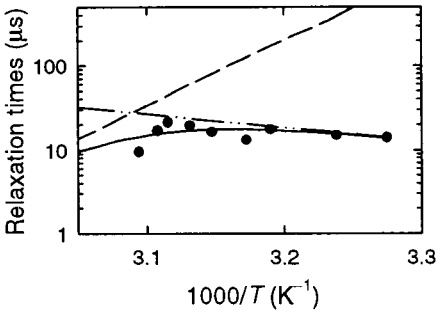

Figure 7. The measured relaxation times versus inverse temperature. The symbols are the experimental data points obtained from exponential fits to the relaxation kinetics. The continuous curve is a fit assuming a two-state approximation with Arrhenius temperature dependence for the closing times (dashed−dot-dot line) and the opening times (dashed line).

and for formation of β-hairpins[25] and α-helix formation[26] in polypeptides. In each of these examples the free energy barrier is primarily entropic with the transition state along an effective one-dimensional reaction coordinate having a lower enthalpy than the random coil state. In the case of hairpin formation in ssDNA, the value of ΔH_c is comparable to the enthalpy gain upon forming a loop,[9] and is consistent with the identification of the transition state as an ensemble of looped conformations with at most one base-pair closing the loop.[18]

A lower enthalpy for the transition state is also predicted from the temperature dependence of the free energy barrier calculated from the results of the equilibrium "zipper" model.[18] In this calculation free energy profiles $G(\theta_I)$, where θ_I is an effective reaction coordinate defined as the fraction of intact base-pairs ($\theta_I = 1 - \theta$), are constructed at each temperature from the statistical weights of all the microstates (defined in eq 2). Here $G(\theta_I) = -RT\ln(p(\theta_I))$, where $p(\theta_I)$ is the Boltzmann probability that the hairpins have a given value of θ_I. The free energy profiles for the hairpin 5′-CGGATAA(T_8)TTATCCG-3′ are plotted in Figure 8a and exhibit a maximum value when the reaction coordinate has a value $\theta_I \approx 1/N_s$, i.e., one base-pair is formed to close a loop. The closing times τ_c are proportional to $\exp(\Delta G^{\ddagger}/RT)$ where $\Delta G^{\ddagger}$ is the height of the free energy barrier, $\Delta G^{\ddagger} = G(\theta_I \approx 1/N_s)$. Therefore, the slope on an Arrhenius-like plot of $\Delta G^{\ddagger}/RT$ versus inverse temperature will yield $\Delta H^{\ddagger}/R$, where $\Delta H^{\ddagger}$ is a measure of the enthalpy of the transition state relative to the random coil state (Figure 8b). This analysis yields values of $\Delta H^{\ddagger} = -10.5 \pm 1.5$ kcal/mol, in remarkable agreement with the value of ΔH_c obtained from kinetics measurements. This agreement between theory and experiment provides support for the accuracy of the parameters obtained from the modeling of the equilibrium data, as well as for the validity of the free energy profiles generated from the equilibrium statistical mechanical calculations.

Comparison with FCS Measurements. Libchaber and co-workers[20,21] have measured the hairpin-to-coil transition by measuring the fluctuations of DNA hairpins, labeled with a fluorophore and a quencher at the two ends, using FCS techniques. They observe single-exponential relaxations for the decay of the fluctuation correlation signals with characteristic relaxation times very similar to the T-jump measurements. However, the dependence of the opening and closing times on temperature and loop size obtained from their measurements is in apparent contradiction with those obtained from our T-jump measurements. First, their measurements show that the closing times scale with the loop size with a slightly higher exponent of ≈2.6 and that there is no dependence of the opening times on the loop size.[20] Second, they find that the activation energies

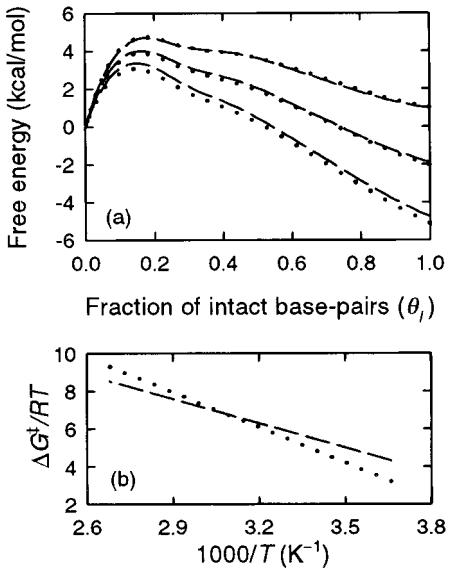

Figure 8. (a) The free energy profiles $G(\theta_I,T)$ for the hairpin with $N = 8$ poly(dT) bases in the loop. The parameters describing the end-loop weighting function correspond to σ_{loop} as defined in eq 4 (dashed lines) and as defined in eq 5 (dotted lines). The three sets of curves correspond to three temperatures: lower curves, 25 °C; middle curves, 40 °C; upper curves, 55 °C. (b) $\Delta G^{\ddagger}/RT$ versus inverse temperature where $\Delta G^{\ddagger}$ is the free energy barrier and is calculated from $G(\theta_I \approx 1/7)$. The slope on this graph is proportional to the enthalpy of activation ($\Delta H^{\ddagger}$); the values of $\Delta H^{\ddagger}$ are −8.5 kcal/mol (dashed line) and −12.3 kcal/mol (dotted line), for σ_{loop} expressed as in eq 4 and as in eq 5, respectively.

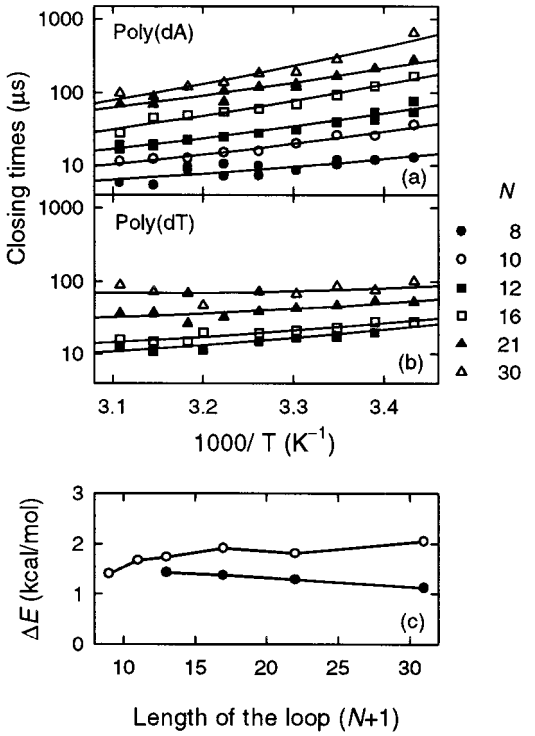

Figure 9. Fits to the closing times using the configurational diffusion model. (a,b) The closing times τ_c are plotted versus inverse temperature. The data are digitized from Goddard et al.[21] for hairpins with (a) poly(dA) loops and (b) poly(dT) loops. The continuous lines through the data points are calculated using the configurational diffusion model, as described in the text, with D_0 and ΔE as free parameters for each hairpin. (c) The amplitude of the roughness ΔE is plotted versus the length of the loop ($N + 1$) for (○) poly(dA) loops and (●) poly(dT) loops.

for the closing times for hairpins with loops similar to the present study are positive (≳5 kcal/mol).[21] Third, their results show significant differences between hairpins consisting of poly(dT) loops and those with poly(dA) loops, with the latter exhibiting an increase in the activation energy with increasing loop size, from ≈5 kcal/mol for loops of $N = 4$ bases to ≈15 kcal/mol for loops of $N = 30$ bases. Fourth, their data indicate deviations from a simple Arrhenius temperature dependence for the closing times (Figure 9).

In a separate series of FCS measurements on hairpins with $N = 30$ poly(dA) bases in the loop, obtained in the laboratory of Klenerman and co-workers, the decay of the fluctuation correlation signals were found to be distinctly nonexponential.[27] More recently, this group has confirmed the deviations from Arrhenius temperature dependence for the closing times; they find negative activation energies for $T \gtrsim T_m$ and slightly positive values for $T < T_m$.[28]

It is important to note here that, to equate the observed activation energies, which are derived from slopes on Arrhenius plots, with the actual activation enthalpy for the transition, requires at least two assumptions: one, that the enthalpy and entropy changes associated with the transition are temperature independent, and two, that the effective diffusion coefficient in the preexponential term is also temperature independent. A significant change in heat capacity has been observed upon DNA melting,[48,49] indicating that the first assumption is not strictly true. In addition, as we show in the following discussion, the diffusion coefficient itself may be strongly temperature dependent, leading to positive values for the (apparent) activation energies, even when the enthalpy of the transition state is lower than that of the random coil.

Configurational Diffusion and Transient Trapping. Previously, we have argued that the folding dynamics of hairpins is slowed by transient trapping in misfolded states arising from incorrect nucleation in which base-pairs are formed with mismatched stems or as a result of hydrophobic interactions between exposed bases.[22,30] A similar argument was put forth by Klenerman and co-workers, who postulated that intrachain interactions, specially stacking interactions in the loop, result in a slowing down of the intramolecular chain diffusion.[28] The fact that ssDNA chains tend to be "sticky" is also evident from single-molecule stretching experiments on ssDNA that show deviations from the force-extension curves expected for simple polymers[44] and which can be explained by local hairpin formation in the limit of low forces.[45] Here we show that we can quantitatively reproduce the temperature dependence for the closing times observed in the measurements of Goddard et al.,[21] and reconcile many of the differences between our T-jump measurements and the FCS measurements of Libchaber and co-workers if we postulate that transient trapping in misfolded loops decreases the effective configurational diffusion coefficient describing the dynamics of hairpins along the free energy profiles shown in Figure 8a.

The conceptual framework behind the configurational diffusion model was developed in the context of a statistical mechanical description of the kinetics of protein folding.[50−53] The kinetics can be described as diffusion along an effective one-dimensional reaction coordinate with the configurational diffusion coefficient rescaled by a factor $\exp(-(\Delta E/RT)^2)$as a result of local trapping or local "roughness" in the free energy profiles of magnitude ΔE.[54−56] Therefore, the temperature dependence of the closing times have contributions from both the changes in the free energy profiles as well as the changes in the effective diffusion coefficient with temperature. The latter has contributions from the temperature-dependent change in the

viscosity (which accounts for ≈4 kcal/mol in the apparent activation energy in aqueous solutions and which was not included explicitly in the analysis of Libchaber and co-workers) as well as from the roughness of the energy landscape, and which contributes an additional $(\Delta E)^2/RT$ to the activation energy. The roughness is expected to increase as the temperature decreases. We therefore postulate that at temperatures $T < T_m$, which is the primary range of the FCS measurements of Libchaber and co-workers, the positive contribution from $(\Delta E)^2/RT$ outweighs the intrinsic lower enthalpy of the transition state, resulting in positive values for the observed activation energy.

More precisely, we use the equilibrium "zipper" model to enumerate all possible microstates of the system (eq 2), with the end-loop weighting function for each microstate with n unpaired bases in the loop given by $w_{loop}(n)$ (eq 3). We then construct free energy profiles $G(\theta_I)$ along the effective reaction coordinate θ_I as a function of temperature (Figure 8a). The corresponding values of the closing times are calculated from the double integral expression:[54,57]

$$\tau_c = \int_0^1 d\theta_I \int_0^{\theta_I} d\theta_I' \frac{\exp[\beta G(\theta_I) - \beta G(\theta_I')]}{D(\theta_I)} \qquad (8)$$

where $\beta = 1/RT$ and $D(\theta_I)$ is the coordinate-dependent diffusion coefficient. $D(\theta_I)$ is assumed to have the following temperature dependence:[22]

$$D(\theta_I,T) = D_0\left(\frac{T}{T_0}\right)\left(\frac{\eta(T_0)}{\eta(T)}\right)\exp\left[-\left(\frac{\Delta E}{RT}\right)^2\right] \qquad \theta_I < \theta_T \quad (9a)$$

$$D(\theta_I,T) = D_0\left(\frac{T}{T_0}\right)\left(\frac{\eta(T_0)}{\eta(T)}\right) \qquad \theta_I \geq \theta_T \quad (9b)$$

where D_0 is the intrinsic diffusion coefficient at the reference temperature T_0 in the absence of any trapping, ΔE is the roughness in the free energy profiles as a result of transient trapping, and θ_T ($=1/N_s$) is the location of the transition state corresponding to the formation of one correct base-pair. In the formulation of eq 9 we assume that the traps decrease the effective diffusion coefficient prior to the nucleation step ($\theta_I < \theta_T$) and that once the correct base-pair is formed, the "zipping" progresses downhill with no further trapping. In describing the temperature dependence of the closing times, two parameters are varied: D_0 and ΔE. This simple model adequately describes the closing times obtained by Goddard et al., including the slight deviations from Arrhenius temperature dependence (Figure 9a,b). Most importantly, the model reconciles the positive activation energies for the closing step at $T < T_m$ (as derived from the positive slopes of $\ln(\tau_c)$ versus $1/T$ plots of Goddard et al.) with the intrinsic lower enthalpy of the transition state obtained from the temperature dependence of the underlying free energy profiles (Figure 8), and from our T-jump measurements at $T \approx T_m$ (Figure 7). The results of this analysis are also consistent with the observations of Wallace et al.;[28] they observe significant deviations from Arrhenius temperature dependence and a change in the sign of the activation energy for the closing step with a crossover near T_m.

An interesting corollary of the configurational diffusion model is that the observation of Libchaber and co-workers, that the scaling exponent describing the closing times versus the length of the loop increases from about 2.3 to 2.9 as the temperature decreases from about 33 °C to about 10 °C,[20] can be explained, at least qualitatively. The exponent observed in the FCS measurements for $T < T_m$ are larger than the exponent of 1.8 expected from applying a flexible polymer model for loop-closure probability and is symptomatic of the fact that at low temperatures, larger loops are slowed more because of a greater probability of getting trapped in misfolded loops. In T-jump measurements for which $T \approx T_m$, the probability of trapping decreases, and the measured exponent of 2.0 ± 0.2 approaches that expected from polymer theories. At present we cannot explain why Libchaber and co-workers do not observe any loop dependence to their opening times except to suggest that the equilibrium constants that they use in order to calculate the opening and closing times, which are calculated from equilibrium melting profiles obtained from fluorescence measurements, may not reflect the true fraction of open and closed states. It has been shown previously that fluctuations in the fluorescent probe can lead to apparent melting profiles that are shifted to lower temperatures relative to the absorbance profiles.[22,58]

Energetic Cost of Bending the Chain. In the analysis of Libchaber and co-workers, they find that the enthalpic cost of forming poly(dA) loops increases with the length of the loop and attribute it to the increased propensity for poly(dA) to stack. In their model, longer poly(dA) strands require more bases to be unstacked in order to form a loop, resulting in an increase in the activation energy. This result runs counter to the expectation that the energetic cost of bending the chain should in fact decrease as approximately $1/L$.

In a very simple, albeit instructive, description of loop formation in a chain consisting of N bases (and $N + 1$ links), such that the angle between two successive links is $\delta \approx 2\pi/(N + 1)$, the energetic cost for bending the chain into a loop of length $L = (N + 1)h$ can be written as

$$E_b \approx \sum_{i=1}^{N} {}^1/_2 g_b \delta^2 \approx \frac{2\pi^2 g_b}{N+1} \qquad (10)$$

Here g_b is the bending energy constant in units of energy/radian and is related to the persistence length of the chain. Equation 10 shows that the energetic cost of bending a chain should decrease as $1/L$. It is therefore not intuitive that the energetic cost of forming loops should increase with loop length, even for poly(dA) strands which are known to exhibit significantly more stacking than poly(dT) strands. The measurements of Felsenfeld and co-workers, on the scaling of the radii of gyration and intrinsic viscosity with the length of the single-stranded polynucleotides under "theta-solvent" conditions, show that the molecular dimensions of long single-stranded poly(rU) and poly(rA) polymers scale as expected from theories of semiflexible polymers.[40,46] Furthermore, these measurements reveal a significant temperature dependence of the radius of gyration of poly(rA) strands as a result of considerable stacking of the adenine bases at lower temperatures. Therefore, although we should expect differences in the intrinsic flexibility of poly(dT) and poly(dA) strands, a greater extent of stacking in poly(dA) strands should result primarily in an increase in the effective persistence length of poly(dA) strands compared to poly(dT) strands, and not in an increase in the energetic cost of bending the chain into a loop for longer length loops, as suggested by Libchaber and co-workers.

In our configurational diffusion model, an increase in the observed activation energy with increasing loop size is accounted for by an increase in the effective roughness ΔE (Figure 9c). The result that ΔE increases with the length of the loop for poly(dA) strands and not for the poly(dT) loops is explained by postulating that poly(dA) strands, with their increased propensity to stack, can also misstack and form "molten globule"

like structures, and that the probability of such misfolds increases as the length of the poly(dA) strands increases. A similar interpretation has been offered by Klenerman and co-workers[28] who postulate that the considerable slowing down of the kinetics for hairpins with large (N=30) poly(dA) loops, in comparison with hairpins with poly(dT) loops, is a consequence of the increased intrachain interactions because of stacking interactions among the adenine bases and which lead to an increased roughness in the free energy landscape of hairpins with poly(dA) loops. A characteristic roughness ΔE would result in a decrease in the effective configurational diffusion constant and a corresponding increase in the closing times by a factor of $\exp((\Delta E/RT)^2)$, which varies from ≈17 for $\Delta E = 1$ kcal/mol to ≈90 000 for $\Delta E = 2$ kcal/mol, at ≈25 °C.

Diffusion-Limited Contact Times for Loop Closure. Models describing the characteristic time for two ends of a polymer chain to come into contact have been proposed in several theoretical studies.[57,59−63] Here we present an order-of-magnitude estimate for ssDNA and compare it with the experimental measurements of the characteristic time for hairpin formation. The diffusion-limited time for the two ends of the chain to come together is estimated as $\tau_D \approx \langle r^2\rangle/2D_T$ where D_T is the translational diffusion coefficient of the chain and $\langle r^2\rangle$ is the mean-square end-to-end distance.[64] We can estimate the translational diffusion coefficient from$D_T \approx k_BT/(6\pi\eta R_G)$ where η is the solvent viscosity and R_G is the radius of gyration $R_G^2 \approx \langle r^2\rangle/6$.[29] Therefore,

$$D_T \approx \frac{k_BT}{6\pi\eta\langle r^2\rangle^{1/2}/\sqrt{6}} \approx 0.13\frac{k_BT}{\eta\,\langle r^2\rangle^{1/2}} \qquad (11)$$

and the diffusion-limited contact time becomes

$$\tau_D \approx \frac{\eta\,<r^2>^{3/2}}{0.26k_BT} \qquad (12)$$

The result in eq 11 is very similar to the result of Szabo et al.[57] who write $\tau_D = \langle r^2\rangle^{3/2}/4D_Ma$ where D_M is the monomer diffusion coefficient and a is the contact distance which may be approximated as the radius of a monomer. Therefore, if we write $D_Ma \approx k_BT/6\pi\eta$, we recover eq 12 to within a small difference in the numerical constant.

For a wormlike chain the mean-square end-to-end distance $\langle r^2\rangle$ can be written as[65]

$$\langle r^2\rangle = 2PL[1 - (P/L)(1 - \exp(-L/P))] \qquad (13)$$

where P is the persistence length of the chain and L is the contour length. For a loop of N ≈10 nucleotides, the length of the loop $L \approx (N + 1)h \approx 5.7$ nm. Using $P \approx 1.4$ nm yields $\langle r^2\rangle \approx 12.1$ nm^2. Therefore, for $T = 25$ °C and $\eta = 1$ cP, we obtain $D_T \approx 1.5 \times 10^{-6}$ cm^2/s. An independent estimate of the translational diffusion coefficient and hence a check on our order-of-magnitude calculation is obtained by scaling the measured value of the diffusion coefficient for a long single-stranded chain, using $D_T \sim 1/\sqrt{N}$. Wetmur and Davidson[66] report a value of $D_T = 1.9 \times 10^{-8}$ cm^2/s for a single-stranded polynucleotide with 3.8×10^4 nucleotides. Therefore, for a strand of about 10 nucleotides, we obtain $D_T \approx 1.1 \times 10^{-6}$ cm^2/s, in close agreement with our theoretical estimate.

The diffusion-limited contact time is estimated from eq 12 to be $\tau_D \approx 40$ ns at 25 °C. There are no direct experimental measurements on the characteristic times for contact formation between two ends of a ssDNA chain. However, experimental measurements have been made on contact formation between two ends of a polypeptide chain, using triplet−triplet energy transfer requiring van der Waals contact between the donor and the acceptor molecules located at the ends of polypeptide chains of varying lengths.[67,68] These measurements yield values of about 50−100 ns for contact formation when the contour length is about 10-residues long. The characteristic persistence lengths for polypeptides may vary depending on the sequence.[69] Bieri et al.[67] estimate a persistence length of about 3 amino acids for their polypeptide. Our estimate of $P \approx 1.4$ nm for poly(dT) strands in ssDNA, together with an estimate of ≈0.52 nm for the internucleotide distance, yields $P \approx 2.7$ nucleotides for ssDNA. Therefore, the time-scales for contact formation are not expected to be very different for the two polymers with similar number of monomers.

The closing times for hairpin formation in ssDNA are estimated to be ≈10 μs at 25 °C for hairpins with about 10 bases in the loop. The diffusion-limited time for contact formation in ssDNA is therefore smaller than the observed closing times by a factor of ≈ 250. It is interesting to note that the time-scales for β-hairpin formation in polypeptides are also found to be several microseconds long:[25] about 2 orders of magnitude larger than the corresponding diffusion-limited contact times in polypeptides.[67,68] Finally, it is well-known that cyclization times for λ DNA molecule with cohesive ends are also much larger than the diffusion-limited times.[70−72]

In the cyclization studies of λ DNA, Wang and Davidson argued that the rate- determining step in the joining of the two ends is a "chemical" step of base-pair formation.[70−72] They found that the temperature dependence of the measured cyclization times exhibited a very large (≈24 kcal/mol) activation energy. Furthermore, they showed that the viscosity dependence of the cyclization times did not follow a simple scaling with solvent viscosity as expected for a diffusion-controlled reaction.[71,72] Wallace et al.[28] have measured the viscosity dependence of the conformational fluctuations of a DNA hairpin and report that the opening and closing times scale nearly linearly with viscosity, with a scaling exponent of ≈0.8. It should be kept in mind that it is not straightforward to interpret the viscosity dependence of measured relaxation times since the addition of viscogenic solvents changes quite significantly the stability of duplex formation.[72] It is therefore not obvious whether the origin of the discrepancy between the diffusion-limited contact times for loop closure and the observed times for hairpin formation is the same as that for DNA cyclization. Our configurational diffusion model with transient traps gives an alternative explanation for the observed discrepancy. As discussed earlier, an increase in the "roughness" ΔE from 1 to 2 kcal/mol would increase the characteristic closing times by a factor of ≳4000. Therefore, misfolded loops that act as dead ends in the zipping process can easily account for the difference between the diffusion-limited contact time (τ_D) and the characteristic time for hairpin formation (τ_c) that occurs only after the correct nucleating contact is made.

Conclusions

We have obtained the characteristic times for formation of nucleating loops that lead to subsequent "zipping" of hairpins as a function of the loop size. Our results show that the hairpin closing times scale with the length of the loop with an exponent of ≈2.0 ± 0.2 near the melting temperatures, in close agreement with the scaling exponent of 1.8 expected from polymer theories. The apparent differences in the scaling exponent obtained in our measurements and those from the work of Libchaber and co-workers[20] are accounted for by postulating that at low

temperatures the dynamics are dominated by configurational diffusion among conformations with misfolded loops before the correct nucleation that results in rapid "zipping" of the hairpin. The more than 2 orders of magnitude discrepancy between the hairpin closing time ($\approx$10 μs) and the diffusion-limited time for contact formation ($\approx$40 ns), estimated at 25 °C for hairpins with about 10 bases in the loop, is explained in the context of the configurational diffusion model in which the rate-determining step for closing hairpins is the formation of a correct nucleating loop. It will be important to directly measure the characteristic time for contact formation between two ends of a ssDNA, as has been measured for polypeptides.

Our configurational diffusion model also quantitatively explains the observation that activation energies for the closing step are found to be negative at high temperatures and positive at low temperatures, as a result of increased trapping at low temperatures. The model highlights the fact that a simple two-state analysis with Arrhenius temperature dependence, although adequate for a narrow temperature range near the melting temperature, is not sufficient to describe the kinetics over a wide range in temperatures. A more complete analysis of the relaxation kinetics would come from a statistical mechanical "kinetic zipper" model as in the description of the kinetics of duplex formation[23,24] but including the possibility of misfolded loops.

Acknowledgment. We have benefited from discussions with Albert S. Benight, John F. Marko, and Alexander Vologodskii. A.A. acknowledges support from National Science Foundation, through grants MCB-9707480 and MCB-9722295, and from the donors of the Petroleum Research Fund, administered by the American Chemical Society, through Grant ACS-PRF 32099-AC4.

References and Notes

(1) Roth, D. B.; Menetski, J. P.; Nakajima, P. B.; Bosma, M. J.; Gellert, M. *Cell* **1992**, *70*, 983.
(2) Bhasin, A.; Goryshin, I. Y.; Reznikoff, W. S. *J. Biol. Chem.* **1999**, *274*, 37021.
(3) Kennedy, A. K.; Guhathakurta, A.; Kleckner, N.; Haniford, D. B. *Cell* **1998**, *95*, 125.
(4) Scheffler, I. E.; Elson, E. L.; Baldwin, R. L. *J. Mol. Biol.* **1968**, *36*, 291.
(5) Scheffler, I. E.; Elson, E. L.; Baldwin, R. L. *J. Mol. Biol.* **1970**, *48*, 145.
(6) Gralla, J.; Crothers, D. M. *J. Mol. Biol.* **1973**, *73*, 497.
(7) Uhlenbeck, O. C.; Borer, P. N.; Dengler, B.; Tinoco, I., Jr. *J. Mol. Biol.* **1973**, *73*, 483.
(8) Hilbers, C. W.; Haasnoot, C. A.; de Bruin, S. H.; Joordens, J. J.; van der Marel, G. A.; van Boom, J. H. *Biochimie* **1985**, *67*, 685.
(9) Haasnoot, C. A.; Hilbers, C. W.; van der Marel, G. A.; van Boom, J. H.; Singh, U. C.; Pattabiraman, N.; Kollman, P. A. *J. Biomol. Struct. Dyn.* **1986**, *3*, 843.
(10) Senior, M. M.; Jones, R. A.; Breslauer, K. J. *Proc. Natl. Acad. Sci. U.S.A.* **1988**, *85*, 6242.
(11) Zuker, M. *Science* **1989**, *244*, 48.
(12) Paner, T. M.; Amaratunga, M.; Doktycz, M. J.; Benight, A. S. *Biopolymers* **1990**, *29*, 1715.
(13) Paner, T. M.; Amaratunga, M.; Benight, A. S. *Biopolymers* **1992**, *32*, 881.
(14) Rentzeperis, D.; Alessi, K.; Marky, L. A. *Nucleic Acids Res.* **1993**, *21*, 2683.
(15) Serra, M. J.; Turner, D. H. *Methods Enzymol.* **1995**, *259*, 242.
(16) Vallone, P. M.; Paner, T. M.; Hilario, J.; Lane, M. J.; Faldasz, B. D.; Benight, A. S. *Biopolymers* **1999**, *50*, 425.
(17) Paner, T. M.; Riccelli, P. V.; Owczarzy, R.; Benight, A. S. *Biopolymers* **1996**, *39*, 779.
(18) Kuznetsov, S. V.; Shen, Y.; Benight, A. S.; Ansari, A. *Biophys. J.* **2001**, *81*, 2864.
(19) Vallone, P. M.; Benight, A. S. *Nucleic Acids Res.* **1999**, *27*, 3589.
(20) Bonnet, G.; Krichevsky, O.; Libchaber, A. *Proc. Natl. Acad. Sci. U.S.A.* **1998**, *95*, 8602.
(21) Goddard, N. L.; Bonnet, G.; Krichevsky, O.; Libchaber, A. *Phys. Rev. Lett.* **2000**, *85*, 2400.
(22) Ansari, A.; Kuznetsov, S. V.; Shen, Y. *Proc. Natl. Acad. Sci. U.S.A.* **2001**, *98*, 7771.
(23) Porschke, D.; Eigen, M. *J. Mol. Biol.* **1971**, *62*, 361.
(24) Craig, M. E.; Crothers, D. M.; Doty, P. *J. Mol. Biol.* **1971**, *62*, 383.
(25) Munoz, V.; Thompson, P. A.; Hofrichter, J.; Eaton, W. A. *Nature* **1997**, *390*, 196.
(26) Lednev, I. K.; Karnoup, A. S.; Sparrow, M. C.; Asher, S. A. *J. Am. Chem. Soc.* **1999**, *121*, 4076.
(27) Wallace, M. I.; Ying, L.; Balasubramanian, S.; Klenerman, D. *J. Phys. Chem. B.* **2000**, *104*, 11551.
(28) Wallace, M. I.; Ying, L.; Balasubramanian, S.; Klenerman, D. *Proc. Natl. Acad. Sci. U.S.A.* **2001**, *98*, 5584.
(29) DeGennes, P. G. *Scaling Concepts in Polymer Physics*; Cornell University Press: Ithaca, NY, 1979.
(30) Ansari, A.; Shen, Y.; Kuznetsov, S. V. *Phys. Rev. Lett.* **2001**. In press.
(31) Wartell, R. M.; Benight, A. S. *Phys. Rep.* **1985**, *126*, 67.
(32) Owczarzy, R.; Vallone, P. M.; Goldstein, R. F.; Benight, A. S. *Biopolymers* **1999**, *52*, 29.
(33) Yamakawa, H.; Stockmayer, W. H. *J. Chem. Phys.* **1972**, *57*, 2843.
(34) Shore, D.; Langowski, J.; Baldwin, R. L. *Proc. Natl. Acad. Sci. U.S.A.* **1981**, *78*, 4833.
(35) Hagerman, P. J. *Biopolymers* **1985**, *24*, 1881.
(36) Camacho, C. J.; Thirumalai, D. *Proc. Natl. Acad. Sci. U.S.A.* **1995**, *92*, 1277.
(37) Mills, J. B.; Vacano, E.; Hagerman, P. J. *J. Mol. Biol.* **1999**, *285*, 245.
(38) Metropolis, N.; Rosenbluth, A. W.; Rosenbluth, M. N.; Teller, A. H.; Teller, E. *J. Chem. Phys.* **1953**, *21*, 1087.
(39) Ansari, A.; Jones, C. M.; Henry, E. R.; Hofrichter, J.; Eaton, W. A. *Biochemistry* **1994**, *33*, 5128.
(40) Inners, L. D.; Felsenfeld, G. *J. Mol. Biol.* **1970**, *50*, 373.
(41) Tinland, B.; Pluen, A.; Sturm, J.; Weill, G. *Macromolecules* **1997**, *30*, 5763.
(42) Rivetti, C.; Walker, C.; Bustamante, C. *J. Mol. Biol.* **1998**, *280*, 41.
(43) Smith, S. B.; Cui, Y.; Bustamante, C. *Science* **1996**, *271*, 795.
(44) Maier, B.; Bensimon, D.; Croquette, V. *Proc. Natl. Acad. Sci. U.S.A.* **2000**, *97*, 12002.
(45) Montanari, A.; Mezard, M. *Phys. Rev. Lett.* **2001**, *86*, 2178.
(46) Eisenberg, H.; Felsenfeld, G. *J. Mol. Biol.* **1967**, *30*, 17.
(47) The errors in the fitting parameters are estimated from variation in the parameters that increase the residual sum-of-squares by 50%.
(48) Chalikian, T. V.; Volker, J.; Plum, G. E.; Breslauer, K. J. *Proc. Natl. Acad. Sci. U.S.A.* **1999**, *96*, 7853.
(49) Rouzina, I.; Bloomfield, V. A. *Biophys. J.* **1999**, *77*, 3242.
(50) Bryngelson, J. D.; Wolynes, P. G. *Proc. Natl. Acad. Sci. U.S.A.* **1987**, *84*, 7524.
(51) Leopold, P. E.; Montal, M.; Onuchic, J. N. *Proc. Natl. Acad. Sci. U.S.A.* **1992**, *89*, 8721.
(52) Bryngelson, J. D.; Onuchic, J. N.; Socci, N. D.; Wolynes, P. G. *Proteins* **1995**, *21*, 167.
(53) Socci, N. D.; Onuchic, J. N.; Wolynes, P. G. *J. Chem. Phys.* **1996**, *104*, 5860.
(54) Zwanzig, R. *Proc. Natl. Acad. Sci. U.S.A.* **1988**, *85*, 2029.
(55) Bryngelson, J. D.; Wolynes, P. G. *J. Phys. Chem.* **1989**, *93*, 6902.
(56) Ansari, A. *J. Chem. Phys.* **2000**, *112*, 2516.
(57) Szabo, A.; Schulten, K.; Schulten, Z. *J. Chem. Phys.* **1980**, *72*, 4350.
(58) Xu, D.; Evans, K. O.; Nordlund, T. M. *Biochemistry* **1994**, *33*, 9592.
(59) Wilemski, G.; Fixman, M. *J. Chem. Phys.* **1974**, *60*, 866.
(60) Doi, M. *Chem. Phys.* **1975**, *9*, 455.
(61) Friedman, B.; O'Shaughnessy, B. *Phys. Rev. A.* **1989**, *40*, 5950.
(62) Guo, Z.; Thirumalai, D. *Biopolymers* **1995**, *36*, 83.
(63) Podtelezhnikov, A.; Vologodskii, A. *Macromolecules* **1997**, *30*, 6668.
(64) Winnik, M. A. *Cyclic Polymers*; Semlyen, J. A., Ed.; Elsevier: New York, 1986.
(65) Landau, L. D.; Lifshitz, E. M. *Statistical Physics*, 3rd ed.; Pergamon Press: New York, 1980; Vol. 5.
(66) Wetmur, J. G.; Davidson, N. *J. Mol. Biol.* **1968**, *31*, 349.
(67) Bieri, O.; Wirz, J.; Hellrung, B.; Schutkowski, M.; Drewello, M.; Kiefhaber, T. *Proc. Natl. Acad. Sci. U.S.A.* **1999**, *96*, 9597.
(68) Lapidus, L. J.; Eaton, W. A.; Hofrichter, J. *Proc. Natl. Acad. Sci. U.S.A.* **2000**, *97*, 7220.
(69) Miller, W. G.; Brant, D. A.; Flory, P. J. *J. Mol. Biol.* **1967**, *23*, 67.
(70) Wang, J. C.; Davidson, N. *J. Mol. Biol.* **1966**, *19*, 469.
(71) Wang, J. C.; Davidson, N. *J. Mol. Biol.* **1966**, *15*, 111.
(72) Wang, J. C.; Davidson, N. *Cold Spring Harbor Symp. Quant. Biol.* **1968**, *33*, 409.